Bull Volcanol (2009) 71:1041–1056
DOI 10.1007/s00445-009-0285-7

RESEARCH ARTICLE

Distinguishing volcanic debris avalanche deposits from their reworked products: the Perrier sequence (French Massif Central)

Benjamin Bernard · Benjamin van Wyk de Vries · Hervé Leyrit

Received: 15 February 2008 / Accepted: 24 April 2009 / Published online: 26 May 2009

Abstract Debris avalanches associated with volcanic sector collapse are usually high-volume high-mobility phenomena. Debris avalanche deposit remobilisation by cohesive debris flows and landslides is common, so they can share textural characteristics such as hummocks and jigsaw cracks. Distinguishing original deposits from reworked products is critical for geological understanding and hazard assessment because of their different origin, frequency and environmental impact. We present a methodology based on field evidence to differentiate such epiclastic breccias. Basal contact mapping constrained by accurate altitude and location data allows the reconstruction of deposit stratigraphy and geometry. Lithological analysis helps to distinguish the different units. Incorporation structures, kinematic indicators and component mingling textures are used to characterise erosion and transport mechanisms. We apply this method to the enigmatic sequence at Perrier (French Massif Central), where four units (U1–U4) have been interpreted either as debris flow or debris avalanche deposits. The sequence results from activity on the Monts Dore Volcano about 2 Ma ago. The epiclastic units are matrix supported with an almost flat top. U2 and U3 have clear debris flow deposit affinities such as rounded clasts and intact blocks (no jigsaw cracks). U1 and U4 have jigsaw cracked blocks with matrix injection and stretched sediment blocks. U1 lacks large blocks (>10 m wide) and has a homogenous matrix with an upward increase of trapped air vesicle content and size. This unit is interpreted as a cohesive debris flow deposit spawned from a debris avalanche upstream. In contrast, U4 has large mega-blocks (up to 40 m wide), sharp contacts between mixed facies zones with different colours and numerous jigsaw fit blocks (open jigsaw cracks filled by monogenic intra-clast matrix). Mega-blocks are concentrated near the deposit base and are spatially associated with major substratum erosion. This deposit has a debris avalanche distal facies with local debris flow affinities due to partial water saturation. We also identify two landslide deposits (L1 and L2) resulting from recent reworking that has produced a similar facies to U1 and U4. These are distinguishable from the original deposits, as they contain blocks of mixed U1/U4 facies, a distinctly less consolidated and more porous matrix and a fresh hummocky topography. This work shows how to differentiate epiclastic deposits with similar characteristics, but different origins. In doing so, we improve understanding of present and past instability of the Monts Dore and identify present landslide hazards at Perrier.

Keywords Perrier · Monts Dore · Debris avalanche · Debris flow · Landslide · Deposit texture

Editorial responsibility C. Kilburn

B. Bernard (✉) · B. van Wyk de Vries
Laboratoire Magmas et Volcans, CNRS UMR 6524,
5 rue Kessler,
63038 Clermont-Ferrand, France
e-mail: b.bernard@opgc.univ-bpclermont.fr

H. Leyrit
Direction de l'Enseignement,
Institut Polytechnique Lasalle Beauvais,
rue Pierre Waguet, BP 30313, 60026 Beauvais, France

Introduction

Volcanic rockslide–debris avalanche deposit characteristics and reworking processes

A volcanic rockslide–debris avalanche is generated by volcanic sector collapse and begins as a rockslide that

progressively disintegrates on steep edifice slopes (Voight et al. 1981; Siebert 1984; Glicken 1996). Sector collapse can be linked to the interaction of two mechanisms (McGuire 1996): edifice weakening (erosion, hydrothermal alteration, asymmetric growth) and a triggering mechanism (eruption, earthquake, cryptodome intrusion, heavy rain). Sector collapses are low-frequency high-volume events, commonly with volumes greater than 0.1 km^3 (Siebert et al. 1987). Volcanic debris avalanches cover hundreds of kilometre squared with velocities greater than 100 m/s and have run outs up to 70 km (Siebert 2002). Debris avalanche deposits are heterogenic and poorly sorted (micron—10's m) epiclastic breccia. Jigsaw crack blocks and hummocky topography are their most recognisable characteristics (Siebert 1984). Block and mixed facies are terms generally used to describe debris avalanche deposits (Glicken 1991). Block facies zones are made of large pieces of volcanic edifice that can preserve original source layering (Ui 1983). Mixed facies zones are usually matrix supported and contain clasts of all origins (Glicken 1991).

Volcanic debris flows may derive directly from debris avalanches (Fig. 1) during or a few hours after emplacement, due to increasing water content (water incorporation, snow/ice melt; Palmer et al. 1991; Glicken 1996; Kerle and van Wyk de Vries 2001). They also can result from the breaching of debris avalanche deposit-induced lakes (Costa and Shuster 1988). Such collapse-induced debris flows are typically clay rich and cohesive (Vallance 2000), so their deposits can share textural characteristics with debris avalanche deposits, such as preservation of jigsaw cracks (Capra and Macías 2000; Capra and Macías 2002). As debris avalanche spawned debris flow deposits have facies similar to debris avalanche deposit mixed facies (Glicken 1991), the field evidence commonly used to distinguish

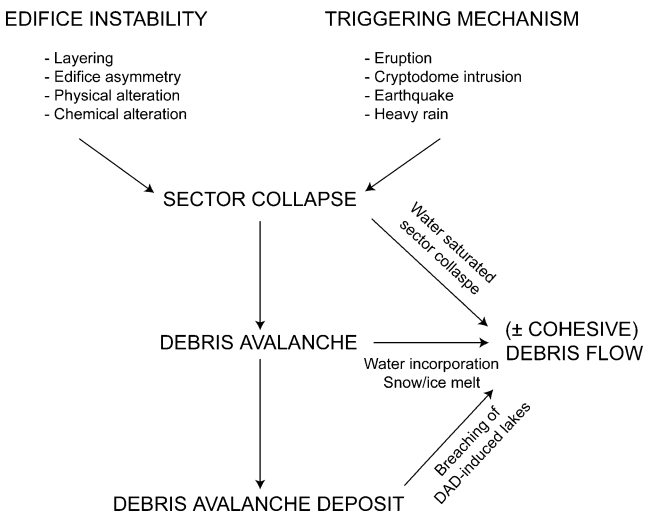

Fig. 1 Schematic diagram illustrating the generation of volcanic sector collapse, debris avalanches and collapse-induced debris flows

both deposits (Ui 1983, 1989; Siebert 1984) cannot be conclusive.

Volcanic debris avalanche deposits are an important source of sediment accumulation at the volcano foot. Their thickness can reach hundreds of metres in narrow valleys (Siebert 1984) and further remobilisation by subsequent landsliding is frequent. Such reworking processes are not yet well studied but show similarities (jigsaw cracks, hummocky topography and facies) between the source and the landslide deposits (Vidal et al. 1996).

Geological hazards on inactive volcanoes

Geological hazards such as rockfalls, landslides and debris flows on dormant or extinct volcanoes can be significant. Over the last century, about 20 small mass movement events are recorded in the Dordogne valley on the Monts Dore Volcano (French Massif Central). Recent debris avalanche deposits are recognised around the volcano such as the Dent du Marais deposit that blocked the Couze Pavin River and created the Lac Chambon natural dam (Vidal et al. 1996). Similar mass movements have affected the neighbouring Cantal volcano, especially occurring in the epiclastic deposits. The Casita (Nicaragua) 1998 landslide also mobilised brecciated epiclastic rocks and turned into a fast-moving debris flow that killed 2,500 people (Kerle and van Wyk de Vries 2001). These examples show that old volcanic and epiclastic deposits, of whatever origin, are susceptible to remobilisation.

Objectives

The distinction between collapse-induced debris flow and debris avalanche deposits in epivolcanic sequences is critical both for understanding volcano evolution (e.g., Etna Volcano, Calvari et al. 1998) and hazard assessment because of their different origin, frequency and environmental impact (Capra et al. 2002). The Perrier Plateau (Fig. 2), French Massif Central, was used as troglodytic dwellings up to a few hundred years ago (Fig. 3). The dwellings are dug in a sequence of epiclastic breccias. These deposits have been interpreted either as debris flow deposits (Ly 1982), debris flow deposits spawned from debris avalanches upstream (Cantagrel and Briot 1990) or debris avalanche deposits corresponding to Monts Dore Volcano collapses 2 Ma ago (Pastre 2004). No in-depth description or discussion has been presented to support these different views. In such an enigmatic area, a sound set of criteria is required to make a reliable interpretation. Thus, we aim to develop an observation-based approach to distinguish the origin and transport mode of each event. We choose to clearly separate each part of the field description (stratigraphy, facies, basal contacts and internal structures)

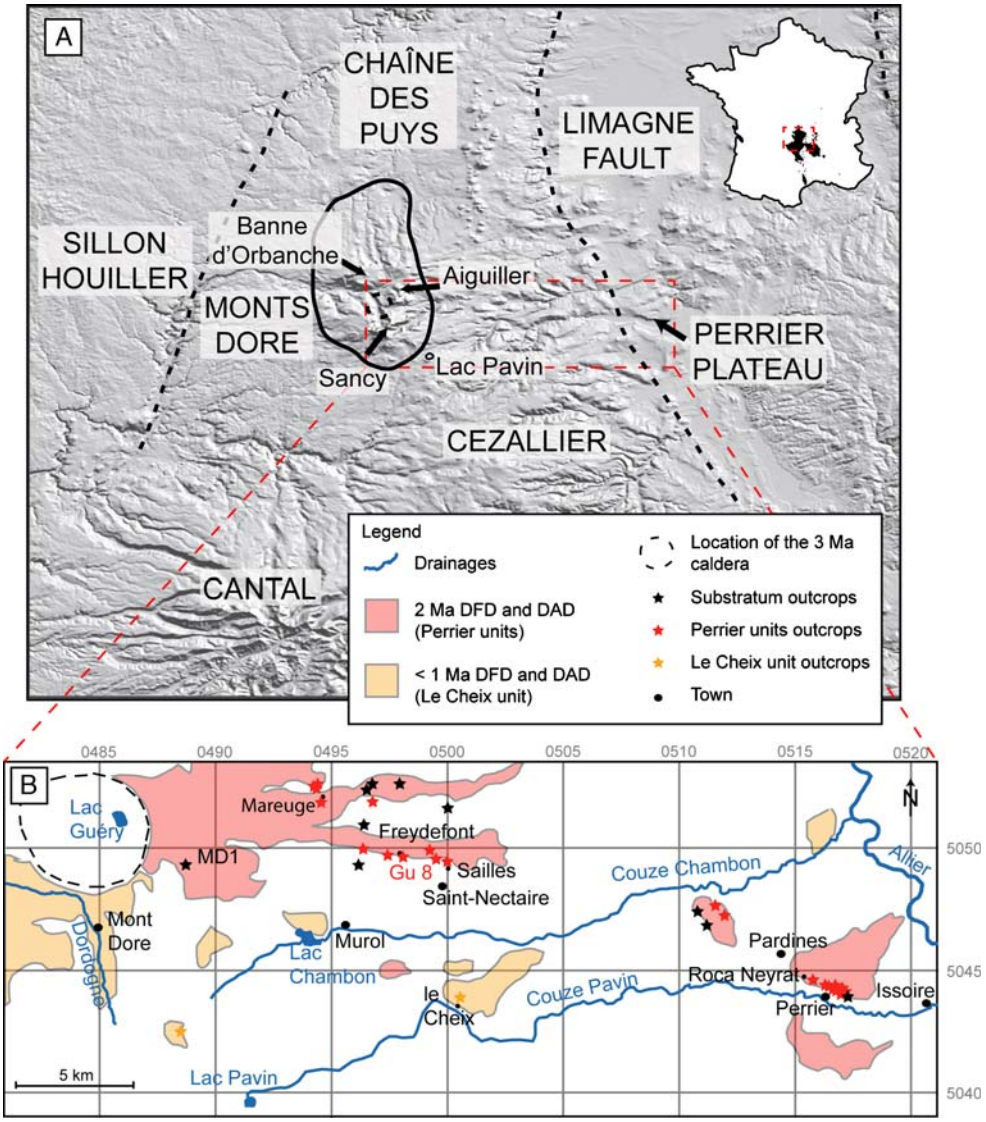

Fig. 2 **a** Shaded relief image of Monts Dore Volcano area (SRTM3 N45E002 and N45E003) and location in the French Massif Central volcanic province (modified from Nehlig et al. 2003); **b** Perrier and le Cheix unit distribution (modified from Cantagrel and Briot 1990)

to give an orderly overview of the deposits. The volcano is regarded as inactive, but landslides are common and additionally, we wish to provide basic geological information for assessment of the present day landslide hazard at Perrier and the Monts Dore Volcano.

Methodology

We used mainly field evidence to distinguish the different units. The deposit geometry and stratigraphy was difficult to observe in the field at close range, due to difficult cliffs or to restricted access areas, but could be extracted from views of the hillside (Fig. 4). Contact altitude and position was extrapolated from one outcrop to another using global positioning system data and an altimeter with a vertical error <3 m. Broad fresh outcrops facilitated the field description of the unit lithologies. The deposits are indurated by 2 Ma of diagenesis so that sieving methods could not be used for granulometry. We used the Glicken (1996) 1-m^2 window method to determine the large clast content (>64 mm) and an equivalent 10-cm^2 method to determine the intermediate clast content (64 mm>Ø> 2 mm). The Glicken (1996) 1-m^2 window method consists of taking a photograph of a 1-m^2 vertical exposure, which presenting a smooth as possible surface. The clasts >64 mm were outlined with vector-based drawing software (Illustrator). The result was analysed with an imaging programme (ImageJ) to extract the clast surface content. As stated in Chayes (1956), the total measurement area is consistent with the clast volume percentage, so we used volume percent. The intermediate clast fraction I (64 mm>Ø> 2 mm) was obtained with the equation:

$$I = I_e \times (1 - L) \quad (1)$$

Fig. 3 Photographs of the Perrier Plateau, with the epiclastic sequence outcrops well exposed by the troglodytic dwellings. **a** The Maurifolet tower in the *left side* is about 25 m high and topped by a tephrite mega-block; **b** view from the southeast of Perrier Plateau; **c** Earth pillar covered by a tephrite mega-block, note the conglomerate inter-bedded between U2 and U4

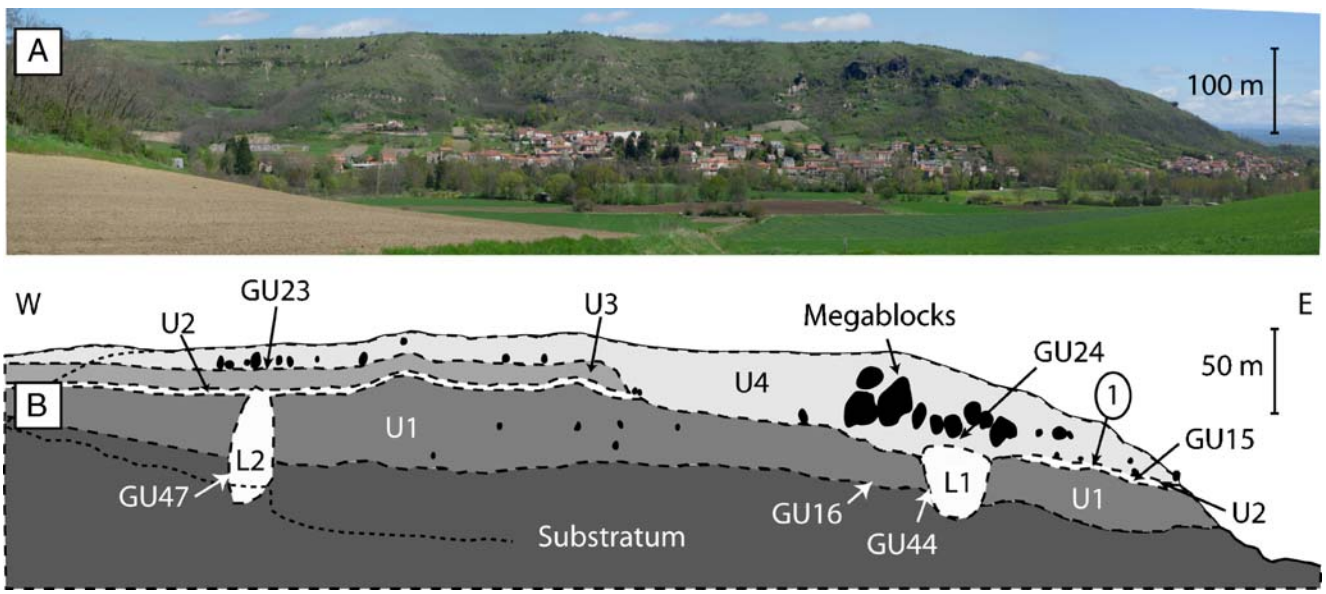

Fig. 4 **a** Panorama of the Perrier Plateau; **b** drawing with a vertical exaggeration of 2 with Perrier epiclastic units (*U1*, *U2*, *U3* and *U4*), main outcrops (*GU*…) and landslide deposits (*L1* and *L2*)

where I = total intermediate clast fraction, I_e = intermediate clast fraction extracted with the 10-cm^2 method and L = large clast fraction.The matrix fraction M (<2 mm) is given by the equation:

$$M = 1 - L - I. \quad (2)$$

We multiplied the windows laterally and vertically to give a facies content average and excluded windows in clasts >50 cm wide that would bias our analysis. We also avoided windows in brecciated blocks. These data were used to determine the unit vertical content (Table 1). The large clast fraction was underestimated, as suggested by Siebert (2002). Nevertheless, the mega-block fraction (>10 m wide) could be interpreted from the panorama (Fig. 4). Matrix composition was qualitatively determined by binocular microscope. We recorded basal contact structures and internal structures. Meaningful structures were systematically photographed and sketched to aid interpretation. Vergence was determined from elongated elements, such as tree trunks and stretched sediments. Erosion and strain-related features at the base of the deposits, such as fractures, inter-leaving and inter-fingering were described and used to constrain the flow rheology. In the deposit interior, we also studied mingling features, such as interpenetration and vertical structures that provide information on the transport mode. The information was finally summarised in a table form that can be used to qualitatively distinguish and compare deposits (Table 2).

The Monts Dore Volcano

The Monts Dore Volcano (longitude, 2.49° E; latitude, 45.35° N) is part of the Neogene Massif Central volcanic province (Fig. 2a). The edifice overlies a Hercynian basement composed of granite and gneiss. It is built between two major faults: the "Sillon Houiller" (NNE–SSW) to the west and the Limagne fault (N–S) to the east. Locally, under the east side of the volcano, the crystalline basement is cut by Permian and Oligocene grabens filled by clay and sandstone. The volcano covers an area of 500 km^2 and has an elliptical shape (35 km N–S and 15 km E–W). Epiclastic products cover a much greater area, especially on the east side of the volcano.

Volcanic activity in the Monts Dore area extends from 20 Ma to 7 ka, including long repose periods. The first signs of volcanic activity, between 20 and 11 Ma, consist of isolated and scattered basanite events (Baudron and Cantagrel 1980). The Monts Dore Volcano *s.s.* activity can be summarised in four stages (Mossand 1983):

1. The pre-caldera volcanism (from 5.5 to 3.2 Ma) consists of large thick basanite lava flows and phreatomagmatic activity, with a few trachytic pyroclastic flows (Ménard 1979).
2. The syn-caldera volcanism (from 3.2 to 2.6 Ma) corresponds to central activity with caldera formation that formed a basin of 20 km^2, 250 m depth (Haute Dordogne Caldera) and produced the >5 km^3 Grande Nappe Ignimbrite, dated at 3.07±0.02 Ma (Vincent 1980; Lo Bello 1988; Duffell 1999).
3. The post-caldera volcanism (from 2.6 to 1.6 Ma) built the Aiguiller massif to the northeast and the Banne d'Ordanche massif to the northwest of the caldera. This stage produced a mainly silica-saturated series with rhyolitic to trachytic lavas separated by under-saturated events. The Aiguiller massif was affected by one or more major collapses during this period, the products of which are well exposed in the Perrier area (Cantagrel and Briot 1990). Between 1.6 and 0.9 Ma, the volcanic activity stopped with only a few basalt flows occurring.
4. The last phase (from 0.9 to 0.25 Ma) attributed to the Monts Dore volcanic complex is the Sancy *s.s.* volcanism south of the old edifice. This activity produced a trachyandesitic stratocone that had periods of intense explosive activity. The Sancy was also affected by a major sector collapse (Le Cheix units; Pastre and Cantagrel 2001). The most recent activity on the Monts Dore are basaltic–trachytic events related to the Chaîne des Puys volcanism, such as the Lac Pavin eruption 7 ka ago (Nehlig et al. 2003). Recently, we have found basalt spatter stuck on glacially formed cliffs that indicate postglacial activity in the central Sancy massif. Landslides and debris flows are common phenomena on the massif, both on the eroded cone and in the peripheral area, notably at the Perrier Plateau (Vidal et al. 1996). Thus, while eruptive activity is currently dormant, unstable volcanic slopes are still active.

Perrier deposits

Geologic context of the Perrier sector

The Perrier Plateau is underlain by Oligocene conglomerates, calcareous marls and clay associated with the Limagne basin. The Perrier section is located near the Allier-Couze Pavin confluence (Fig. 2b). The stratigraphy established by Ly (1982) presents the Perrier Plateau as the result of both volcanic and fluviatile deposition. If we take into account only the volcanic deposits, we can distinguish

Table 1 Lithological data for large clast, intermediate clast and matrix fraction

Unit	Position	Sample	Large clast fraction (>64mm)			Intermediate clast fraction (2mm<ø<64mm)				Matrix fraction <2mm (%)	Non volcanic clasts (%)	Volcanic clasts (%)	Pumice clasts (%)
			Non-volcanic (%)	Volcanic clasts (%)	Total (%)	Non-volcanic (%)	Volcanic clasts (%)	Pumice (%)	Total (%)				
U1	Base	GU16 GRA	0.6	2.0	2.6	0.0	1.9	4.8	6.7	90.7	83.1	29.0	52.3	18.7
		GU16 GRB	10.8	3.3	14.1	0.3	6.3	0.7	7.4	78.5				
		GU16 GRC	6.3	6.7	12.9	0.0	7.9	4.0	11.9	75.1				
		GU16 GRD	0.8	6.8	7.6	0.9	1.9	1.8	4.7	87.7				
		GU16 GRF	4.3	2.7	7.0	0.4	4.6	4.5	9.5	83.5				
	Body	GU26 GRA	2.8	3.3	6.2	0.0	4.0	9.7	13.6	80.2	82.0	14.3	46.1	39.5
		GU26 GRB	1.4	5.1	6.6	0.4	3.9	8.1	12.4	81.1				
		GU26 GRC	0.9	4.5	5.4	2.2	4.1	3.6	10.0	84.6				
	Top	GU27 GRA	7.7	1.6	9.3	0.3	9.4	3.0	12.7	78.0	78.6	17.1	62.2	20.7
		GU27 GRB	1.0	1.0	2.0	3.0	12.5	3.4	18.9	79.0				
		GU27 GRC	0.3	3.3	3.7	0.3	5.5	4.0	9.9	86.5				
		GU27 GRD	0.0	17.0	17.0	3.5	2.8	5.8	12.1	70.9				
		GU30 GRA	0.7	5.5	6.3	3.8	8.2	2.9	14.9	78.8				
		GU30 GRB	0.7	7.2	7.9	0.7	5.9	7.4	13.9	78.1				
U4	Base	GU24 GRA	3.0	15.5	18.4	0.2	8.6	5.0	13.8	67.8	67.6	11.5	68.9	19.5
		GU32 GRA	0.6	14.3	14.8	0.0	4.9	9.4	14.3	70.9				
		GU32 GRB	1.3	17.3	18.6	6.1	6.4	4.6	17.2	64.2				
	Body	GU25 GRA	0.3	15.2	15.5	4.5	2.8	0.0	7.3	77.1	71.2	11.0	82.6	6.4
		GU29 GRA	1.0	16.6	17.6	3.7	7.2	1.5	12.4	70.0				
		GU31 GRA	1.2	14.5	15.7	0.0	7.6	2.8	10.3	74.0				
		GU31 GRB	2.3	14.2	16.5	0.3	13.1	2.8	16.2	67.2				
		GU31 GRC	0.7	15.2	15.9	1.8	12.6	2.1	16.5	67.6				

Pumice clasts are separated from volcanic clasts, because they can come from either the source edifice or the substratum

three different kinds. The older products are lavas from 4.2 to 3.7 Ma (Pardines basanite and Roca-Neyra basalt) associated with the Cézallier volcanoes south of Perrier (Pastre 2004). Rhyolitic plinian fall and pumice flows are encountered coming from the Monts Dore post-caldera activity and dated at 2.4 Ma (Lo Bello 1988). The most recent volcanic products are four epiclastic units. The volcanic events are separated by intense phases of fluviatile incision and deposition that make the Perrier Plateau complex. The erosion creates an apparent inversion of the normal succession putting the Pardines basanite on top of the western part of the plateau. Perrier has also experienced small landslides, such as a 1733 event that reworked part of the Pardines lava and epiclastic products and runout extends for 1,200 m (Vidal et al. 1996). The steepest part of the present Perrier escarpment is now immediately above the village of Perrier.

Spatial extent of the Perrier units

Perrier units are observed sporadically from Perrier to Lac Guery (Fig. 2b). Several outcrops in the proximal region show angular breccias composed of trachyphonolite (MD1, Fig. 2b). Cantagrel and Briot (1990) interpreted these as part of the debris avalanche deposits. We studied these outcrops and find no evidence of transport, so they could also be in situ cataclased domes/intrusions. In the medial area, between Mareuge and St. Nectaire, many small and strongly vegetated outcrops present breccias similar to Perrier units. In the Perrier area, 35 km from source, the southern part of Perrier Plateau gives the best sections of the deposits (Fig. 3). Erosion, vegetation and agriculture have erased or hidden most of the deposits elsewhere.

Stratigraphy

Figures 4 and 5 illustrate the stratigraphy of Perrier Plateau, completing the work of Pastre (2004). Unit 1 (U1) is observed along almost all the Perrier Plateau and has a maximum thickness of 50 m. It overlies a substratum composed of fluviatile layers (F5a in Pastre 2004) and a <0.7-m-thick trachytic plinian fall (RP2 in Pastre 2004) that is partially reworked.

Unit 2 (U2), only 5 to 10 m thick, is observed in the western part, overlain by the Roca-Neyra fossiliferous conglomerates and sands. Its base is now not clearly visible but Pastre (2004) described it on top of a coarse conglomerate. In the eastern part of the plateau, the fluviatile layer composed of pebbles and sand between U1 and U2 reaches 1.8 m thick and reduces to zero towards the east. From west to east, the top of U2 is between 567 and 530 m a.s.l. indicating a very slight slope (~1°). Unit 3 (U3)

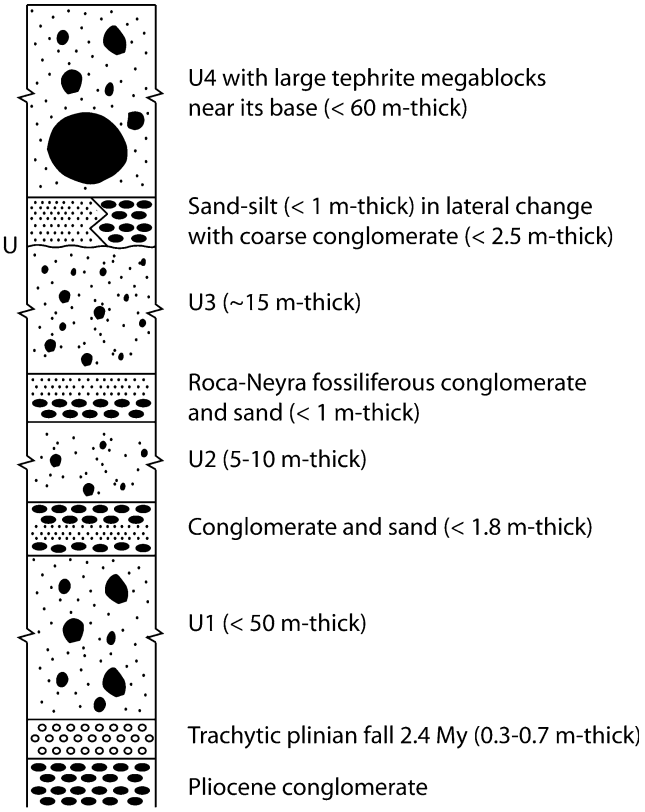

Fig. 5 Schematic stratigraphic column of Perrier Plateau. *U* indicates the main unconformity

is about 15 m thick and is present only in the western part of the plateau.

The unconformity between unit 4 (U4) and the whole sequence indicates a period of incision sufficient to erode more than 25 m of deposits. U4 is the thickest unit (more than 60 m thick) and is present all along the plateau. In the west, U4 overlies U3 with an inter-bedded <1-m-thick distinctive layer of sand-silt with few pebbles. In contrast, in the east, it lies on a coarse conglomerate that has variable thicknesses (from less than 1 m to more than 2.5 m thick) with sometimes a thin layer of sand in between. With the change in substratum, there is a large change of altitude of the U4 base between the eastern and the western plateau. To the west, the base is almost horizontal with an altitude between 577 and 581 m a.s.l. The eastern base has a slight slope (<0.5°) towards the east with altitudes between 539 and 531 m a.s.l. The unconformity observed is likely to be associated with the palaeo-Allier river course.

We found two distinctive breccias (L1 and L2) that were first interpreted as U4-infilled palaeovalleys (Fig. 4). They have fresh hummocky topography and contain a mix of all units. After detailed description and close analysis, they were found to be very recent lobe-like deposits that extend from U4 down to the valley bottom. It is striking, however, the extent to which they closely resemble the old epiclastic

sequence, and this illustrates the difficulty in determining the origin of such breccias. L1 and L2 are interpreted as recent landslides.

Facies description of units

U1

U1 is matrix supported (70–90 vol.% of matrix <2 mm) with some gravel-sized clasts (5–20 vol.% between 2 and 64 mm) and rare blocks (5–15 vol.%>64 mm; Table 1). We noted the absence of mega-blocks (>10 m wide). The matrix contains few lithics (trachyandesite, pumice and marly calcareous sediments) and abundant free crystals (sub-euhedral feldspar, blunt lustrous quartz and mica flakes). The gravel-block fraction is composed of 45 to 65 vol.% trachyandesite and basalt clasts and this proportion increases near the deposit top. There are also fibrous pumice fragments from the Grande Nappe Ignimbrite and vesicular pumice from the trachytic plinian fall (20–40 vol. %). The non-volcanic components are limestone, granite, various pebbles and clay. Their frequency decreases near the deposit top (from 30 to <20 vol.%). The largest block observed (5 m wide) is made of a consolidated pumice deposit (Fig. 6a). U1 has a laterally homogenous mixed facies matrix.

We noted the presence of three kinds of voids in this deposit (Fig. 7):

1. Wood impressions are the most recognisable kind of void left by branches and tree trunks. Some altered wood fragments are still present at depth in the deposit.
2. Closed vesicles are also found. They are smaller than 1.5–2 mm in diameter and constitute 2 vol.% of the deposit. These can locally reach 5 vol.% near the top of U1 where they are up to 6 mm in diameter. The largest vesicles are irregular and horizontally flattened.
3. Pumice clasts require special attention as they fall out and alter to produce false vesicles when a sample is broken, or observed at outcrop. These voids are larger (up to 1.5 cm diameter), regular and rounded (sometimes rectangular when coming from fibrous pumice) and can be confused with closed vesicles.

U2 and U3

U2 and U3 have very similar facies and their contact is marked mainly by a weak layer at their contact that is preferentially eroded. Their facies is very analogous to U1 facies but with a higher matrix content (80–90 vol.%) and therefore fewer blocks. U2 and U3 compositions are similar to U1 but the few exposures do not allow us to make a significant analysis. The maximum size for blocks does not exceed 1 m wide. Most of the clasts are rounded in these units. Both units have high closed vesicle contents (2–3 vol.%, up to 5 mm diameter).

U4

U4 is mainly matrix supported (65–75 vol.% of matrix <2 mm) with some gravel (5–20 vol.% between 2 and 64 mm) and sometimes abundant blocks (15–20 vol.%> 64 mm). The matrix contains a few lithics (trachyandesite, pumice and marls) and abundant free crystals (sub-euhedral to euhedral feldspar, lustrous blunt to rounded quartz and a few ferromagnesians such as mica flakes and amphibole). The gravel-block fraction is composed of ~10 vol.% of material coming from the substratum (marly calcareous sediments, various pebbles and granite fragments) and 70–85 vol.% of material apparently coming from the volcano (mainly trachyandesite and tephrite clasts). The pumice fraction varies from 20 vol. % near the base to 6 vol.% in the body of the deposit. U4 has a variable mixed facies characterised by different colour matrices and gravel-block components. It is worth highlighting the presence of numerous mega-blocks (>10 m wide, up to 10 vol.% of the deposit) that have created beautiful earth pillars (Fig. 3). The largest

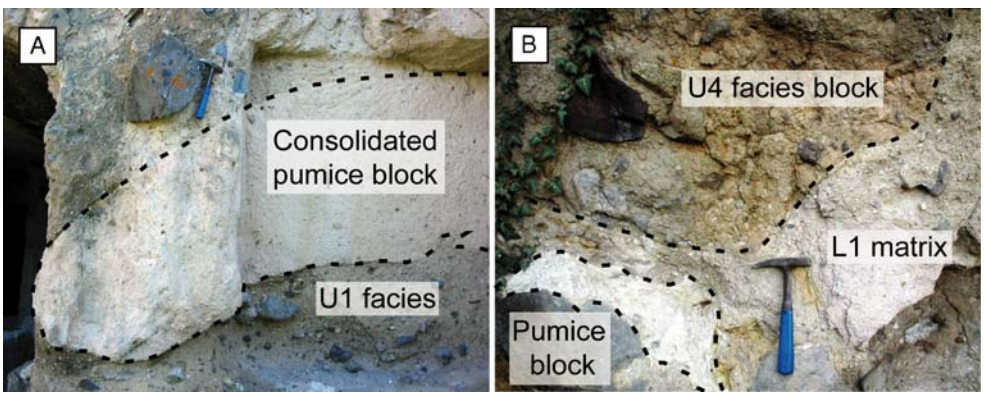

Fig. 6 Perrier deposit typical facies with **a** a large block of consolidated pumice layer within U1 and **b** U4 and stretched pumice blocks within L1. Hammer for scale

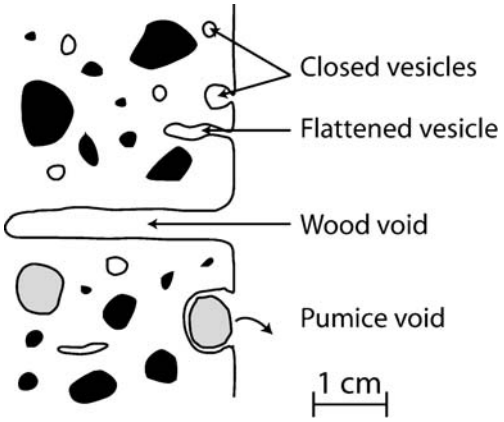

Fig. 7 Section showing different kinds of voids observed in the epiclastic deposits of the Perrier Plateau. Air-trapped vesicles are smaller and more irregular than pumice or wood voids, where it is also possible to observe relics of the original material

mega-blocks are made of tephrite (up to 40 m wide) and are present near the base of the deposit. Locally, the horizontal to oblique stretched blocks are found in groups. This is a common feature observed in typical block facies. The vesicles present in this unit are less than 3 mm in diameter with the edges covered by a thin clay deposit. Their proportion is higher near the base of the deposit (up to 2 vol.%).

L1 and L2

The L1 and L2 units are subtly different from U1 or U4. The facies of these units is slightly more variable than U4 and has a higher porosity. The deposit is more easily crumbled and has less well-developed cementation than the other epiclastic units. L1 is well exposed and contains partially rounded fractured blocks of U1 and U4 facies (Fig. 6b). Distinction between U1 and U4 blocks is based on the lithological content (U1 has greater fibrous and vesicular pumice contents than U4) and the granulometry (U4 is coarser than U1 with large amounts of tephrite blocks). In L2, the distinction between U1, U2 and U3 blocks is difficult because of their similar facies. Large blocks of tephrite material coming from U4 are also found in this deposit. In L1, we would not expect to see U2 and U3 blocks as these units are not present in this area.

Structural analysis

Basal contacts

U1

U1 lies on top of a trachytic plinian fall (RP2 in Pastre 2004) in every outcrop along the east. The sub-planar contact is nearly horizontal and punctuated by small-scale structures (Fig. 8a, b). These include:

1. Oblique (30° N–NNE dip) matrix inter-fingering structures with RP2 (up to 8 cm long)
2. Sub-horizontal (5–10° S to SE dip) incorporation of RP2 by inter-leaving (up to 10 cm long). These features are almost parallel to the contact and point roughly south east, the probable transport direction at this location.
3. Scarce block penetration structures, with usually a planar upper surface and irregular lower side. The blocks are mainly trachyandesite.
4. Discontinuous undulation textures (60–120 cm wavelength and 10–25 cm amplitude).

Rarely, sub-horizontal cleavage-like planar structures are observed near the top of the RP2 layer. Binocular microscope analysis shows that this apparently clean contact at outcrop scale is diffuse at grain scale. No structured grain organisation has been observed in thin section. The contact between RP2 and the underlying sandy alluvium (upper F5b in Pastre 2004) also has inter-fingering and undulation.

Wood voids are present at the contact and in U1. They are elliptical cylinders (long axis: from 3 to 83 cm; maximum diameter: from 2.5 to 16 cm; minimum diameter: from 1.5 to 10 cm) with the long axis almost horizontal near the basal contact and more inclined (up to 30° dip) away from the contact. Of the 14 voids measured, several cannot be used because of their high sphericity ratio, their size, their distance from the basal contact or because they correspond to multiple-branch relics (Fig. 8c). The few acceptable wood void measurements yield a preferential direction between N30 and N65. A clay block deformed around one wood void indicates a southeast deformation vergence, like the inter-leaving structures (Fig. 8d).

U2 and U3

U2 and U3 basal contacts are difficult to observe because they lie in cliff which are difficult to access or are in restricted access areas, but where observed, they are usually sub-horizontal without significant structures.

U4

Basal contacts observed for U4 change markedly along the escarpment. The first kind of contact (e.g., outcrop GU15; Fig. 4) is mostly observed in the east. There, U4 overlies a conglomerate and the contact is sub-horizontal without distinct structures. The conglomerate clasts are not affected by any cataclasis, and the boundary between U4 and the conglomerate matrix is extremely diffuse. There are, in

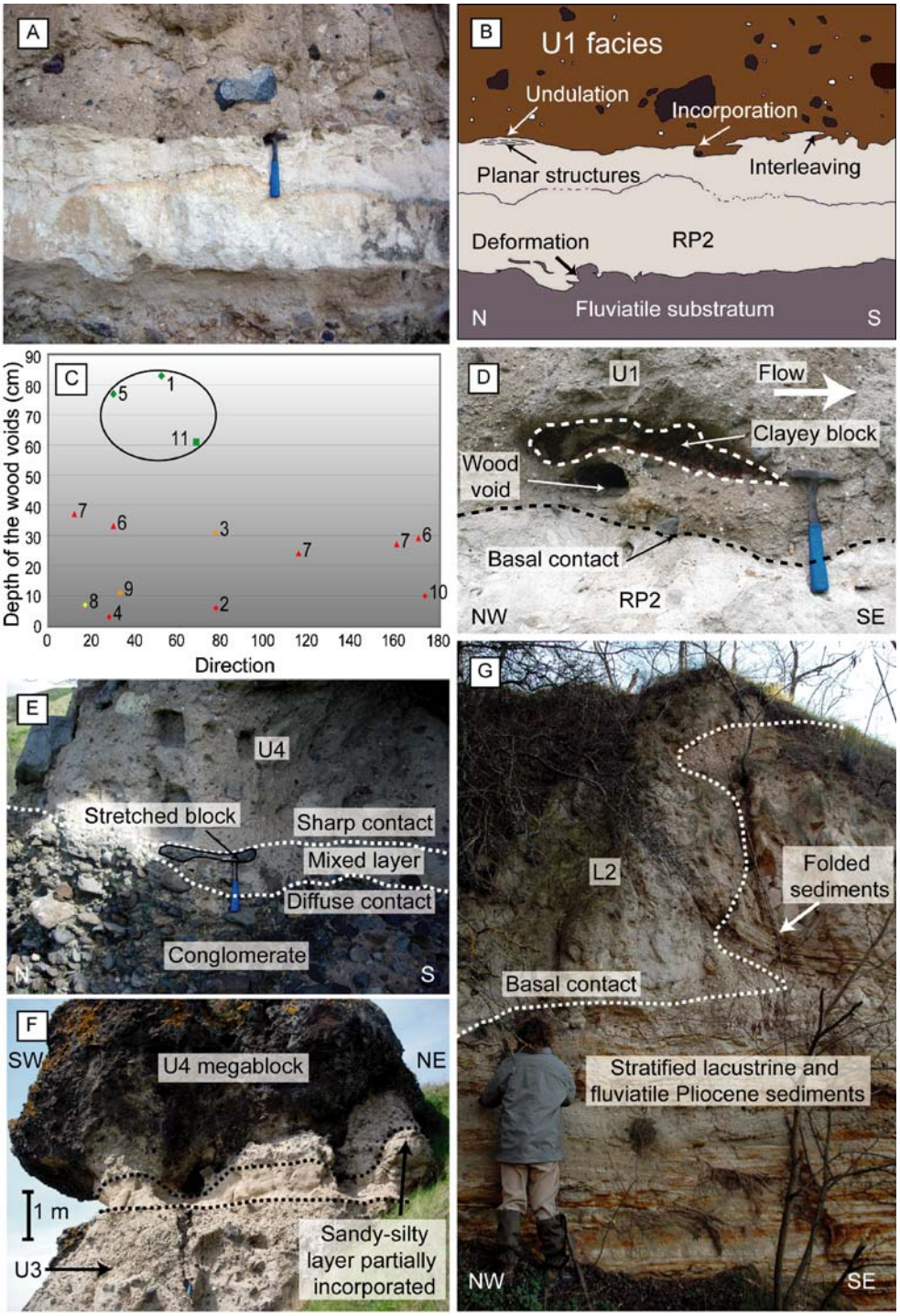

Fig. 8 Basal contacts of Perrier units. **a** Photo and **b** drawing of outcrop GU16 basal contact with several kinds of structures; **c** depth of the wood voids as a function of their orientation in the deposit where voids *2*, *4*, *8* and *10* are excluded because of their size and sphericity ratio; voids *3* and *9* are excluded because they are in the deposit body; voids *6* and *7* correspond to multiple-branch relics; **d** deformed clayey block around a wood void in U1 that shows the flow direction towards the SE (*white arrow*); **e** outcrop GU24 basal contact with the presence of a mixed layer between U4 and the underlying conglomerate; **f** GU23 shows a sandy-silty substratum partially incorporated in U4, probably due to the presence of a tephrite megablock; **g** bulldozer structure observed at the basal contact of L2 (outcrop GU47). Hammer for scale

some places, sub-horizontal cleavage-like planar structures in a <0.2-m-thick sand layer below U4. In the west, this kind of contact is between U4 and a 0.7-m-thick sandy-silty layer (GU23; Fig. 4).

In the GU24 outcrop (Fig. 4), U4 overlies a conglomerate with a planar contact to the west and an irregular and oblique contact to the east. The conglomerate break of slope coincides with the appearance of a distinct layer composed of fine-grained sand and small pebbles with little organisation. Some sub-horizontal planar, elongated, white clasts also appear in this layer that, on close inspection, are seen to be crushed and stretched pumice fragments. The layer thickness reaches a few tens of centimetres. Its contact with the underlying conglomerate is extremely diffuse, whereas the overlying sub-horizontal contact with U4 is sharp and irregular (Fig. 8e). Several pebbles from the

conglomerate are fractured, crushed and aligned following the contact between the two layers. This feature is partially outlined by a thin black layer (0.5 to 1 cm thick) of powder derived from the crushed clasts.

Significant incorporation of the U4 substrata is inferred by the presence of intact conglomerate/sand-silt blocks and mega-blocks in the unit body. In places, usually just below tephrite mega-blocks (Fig. 8f), there is no clearly defined boundary between U4 and U1, indicating that the latter one has been partially remobilised and incorporated.

L1 an L2

Two outcrops (GU44 and GU47; Fig. 4) show clearly the basal contact of L1 and L2. In outcrop GU44, the L1 base is in contact laterally with U1, the trachytic pumice fall and the Perrier coarse alluvium (F5b). The contact has an irregular slope from 15° to 60°. We noted the presence of trachytic pumice dyke-like injections a few centimetres wide and a few tens of centimetres high in L1 that have not been observed in U1 (Fig. 9g). The basal contact is mostly

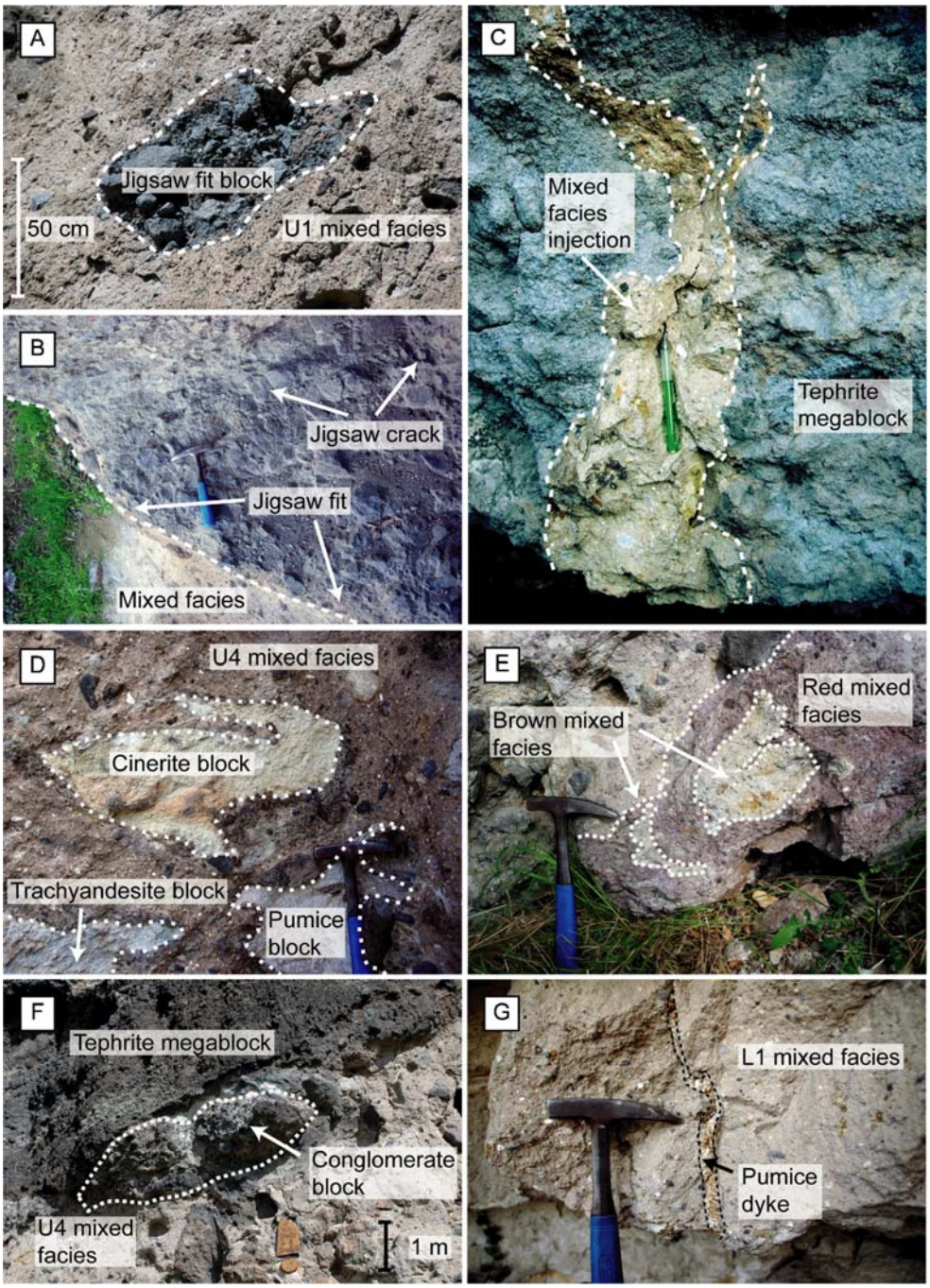

Fig. 9 Internal structures observed in Perrier epivolcanic deposits. **a** Jigsaw fit block in U1; **b** evolution from jigsaw crack in the inner part of the trachyandesite block to jigsaw fit near its boundaries in U4; **c** finger-shaped mixed facies injection in a tephrite mega-block in U4; **d** S-shaped deformation of a fine ash block in U4, note also the deformation of the trachyandesite and pumice blocks; **e** partial mixing between a red mixed facies and a brown mixed facies in U4; **f** unconsolidated conglomerate block under a large tephrite mega-block; **g** pumice dyke in L1 deposit. Hammer for scale

diffuse (from macroscopic to microscopic scale) and no erosive features are observed. In the GU47 outcrop (L2), the Pliocene fluviatile and lacustrine sediments are deformed and overturned (Fig. 8g). This structure is similar to the Belousov et al. (1999) bulldozer structures.

Internal structures

U1, U2 and U3

Few structures have been found in the interiors of U1, U2 and U3. The most notable structure is the horizontal elongation of clayey and marly calcareous blocks (Fig. 8d). In U1, some trachyandesitic blocks have jigsaw cracks and scarce mono-lithologic intra-clast matrix-filled fractures (jigsaw fits; Fig. 9a). No structures are visible within the matrix itself, possibly due to the absence of contrast.

U4

In contrast to the other units, U4 has a large range of structural features. Several sets of striae have been observed on surfaces of trachyandesite and tephrite mega-blocks and in some marls. Regular striated planes do not show a consistent orientation or dip. The striae pitches are usually low (<10°). Trachyandesite and tephrite blocks commonly have jigsaw cracks (Fig. 9b). These fracture frameworks are widespread and hard to quantify. An evolution from jigsaw crack to jigsaw fit is observed from the inner to the outer parts in some blocks. Some blocks and gravel clasts are brecciated and elongated near mega-block boundaries. Mixed facies injections are common in trachyandesite and tephrite blocks, but are scarce in marls and pumice blocks (Fig. 9c). These injections are from a few centimetres to tens of metres in height and from a few centimetres to metres wide. They have finger-shaped terminations and significant vesicle contents (2 vol.%). Marl and pumice layer deformation is often expressed by horizontal elongation and by S-like structures (Fig. 9d). Vortical structures and inter-fingering are observed where different colour matrices (either intra-clast or inter-clast) are present (Fig. 9e). Tilted coherent mega-blocks of unconsolidated conglomerate (up to 10 m wide) are present within U4 and show diffuse boundaries (Fig. 9f).

L1

Low-contrast banding structures with centimetre- to metre-wide spacing are identified in L1 parallel to the basal contact, giving a transport direction towards the southwest. This direction corresponds to the current hill slope. Structures, such as jigsaw cracks, jigsaw fits, and partial mixing of different colour matrices observed in U4 are also recognisable in L1.

Discussion

Cohesive debris flow deposits vs. debris avalanche deposits

Volcanic cohesive debris flow deposits and debris avalanche deposits are both coarse-grained, poorly sorted breccias with a grain size from clay to metric blocks (Siebert 1984; Smith and Lowe 1991; Yarnold 1993; Capra et al. 2002). Typical evidences used to distinguish these deposits are surface morphology and sedimentary architecture (Ui and Glicken 1986; Glicken 1991; Palmer et al. 1991; Vallance 2000). Nevertheless, the progressive transition between both phenomena means that shared features are observed in different origin deposits (Capra et al. 2002). We stress that the presence or absence of one or more individual structural features does not allow a conclusive distinction to be made. Our method, applied to the Perrier deposits, explores all the field evidence incorporating the spatial distribution of features to give the origin of the deposits. Examples of the use of various pieces of evidence are given below:

1. *Deposit thickness:* Debris flow deposits are generally <0 m thick, whereas debris avalanche deposits are commonly up to 100 m thick (Yarnold 1993). In fact, the thickness of the deposit is related to the flow rheology, its volume and the pre-deposit topography (slope and lateral containment). Therefore, large cohesive debris flows can leave deposits up to tens of metres thick, while low-volume debris avalanches can leave deposits of less than 10 m thick (Capra et al. 2002). Thickness, then, is not a conclusive factor.
2. *Terraces and surface morphology*: Debris flow deposits usually form terraces and can show clast-supported streamline lags (Rodolfo 1989), whereas debris avalanche deposits generally present hummocky topography (Ui et al. 2000) or ridged topography (van Wyk de Vries et al. 2001). These surface criteria are not very useful here because such morphological features will have suffered substantial erosion. Furthermore, the deposits are 35 km from the supposed source and have a matrix-supported facies that usually produces a smoother surface morphology in debris avalanche deposits (Glicken 1991).
3. *Matrix characteristics:* A debris flow deposit matrix is homogenous over a large portion of a deposit (Vallance 2000). This fits with the observations made on U1, U2 and U3. In contrast, different colour, mixed facies with sharp contacts and partial mixing structures are common in debris avalanche distal facies

deposits (Siebert et al. 1987; Bernard et al. 2008), and these are clearly observed in U4. The presence or absence of such structures is not sufficient to decide on the origin of the deposits, because our observation is limited to the available outcrops. Moreover, cohesive debris flow deposits spawned from debris avalanches can also have such features (Capra et al. 2002), and debris avalanche marginal facies can have a homogeneous matrix (Palmer et al. 1991).

4. *Vesicle content*: Debris flow deposits may have vesicles as the result of air entrapment (Vallance 2000), as can debris avalanche deposits (Siebert 1984). Trapped air vesicles are generally interpreted as evidence of water saturation of the flow. Their presence in debris avalanche deposits is understood to correspond to a local saturation of the debris avalanches. We observed the vesicles throughout U1, U2 and U3 with vertical content variations. Larger, flattened vesicles could be the result of the deposit compaction after emplacement. Vesicles are locally present in U4, mostly near the base of the deposit.
5. *Erosion and bulking differences:* Debris flows and debris avalanches are erosive phenomena and erosional features at their base are common (Yarnold 1993; Bernard et al. 2008). The fraction of incorporated material can be estimated using the non-volcanic component (15 to 30 vol.% in U1, 10 vol.% in U4) and this proportion reflects a minimum value for incorporation, as pumice and other volcanic clasts can also come from bulking. We observed RP2 pumice incorporation through abrasion in U1. U4 basal contacts also show abrasive structures, but incorporation of large blocks of unconsolidated conglomerate suggests a different erosional mechanism. This kind of bulking is always spatially associated with the tephrite mega-blocks. The persistence of unconsolidated blocks in the unit body implies particular characteristics of the flow such as an elevated cohesion and under-saturation.
6. *Block deformation:* Blocks are present in both debris flows and debris avalanche deposits, but are generally subject to cataclasis only in debris avalanches. Blocks in debris flow deposits can preserve some jigsaw crack blocks as relics of conversion from a debris avalanche (Smith and Lowe 1991). Deformed blocks are observed

Table 2 Debris flow and debris avalanche deposit key characteristics that can be used for distinguishing deposit origin, adapted from (Ui 1983; Siebert 1984; Glicken 1991; Palmer et al. 1991; Smith and Lowe 1991; Yarnold 1993; Vallance 2000; Capra and Macías 2002; Capra et al. 2002)

Deposit type	Debris flow deposits	Debris flow deposits spawned from debris avalanches	Debris avalanche deposits
Texture	Coarse-grained, poorly sorted, heterometric and heterogenic breccias		
Thickness	Dependent of the channel geometry but typically < 10 m thick	Dependent of the channel geometry with common thickness > 15 m	Maximum thickness can be greater than 100 m
Facies	Mixed facies		Mixed and block facies
Matrix characteristics	Homogenous over large portions of the deposits		Sharp contact between different colour matrices
Vesicles	Common with a possible increase in size and content near the top of the deposits		Uncommon and restricted to parts of the deposits
Block fracturing	Uncommon	Scatered jigsaw cracks and fits	Common jigsaw fracturing
Maximum block size	Typically < 10 m in the long dimension, maximum clast size correlates with bed thickness	Dependent of the source material with debris avalanche blocks > 10 m in the long dimension observed	Massive blocks > 10 m^3 are common and shatterred block up to 100 m in the long dimension
Substratum erosion	Large substratum material amount but incorporation piece-by-piece		Large substratum amount with large blocks of unconsolidated substratum material
Internal structures	Few sediment blocks deformation	Sediment blocks deformation and partial mixing between jigsaw fit blocks and the mixed facies	Common sediment and volcanic blocks deformation, partial mixing between blocks and different colour mixed facies
Perrier units	U2 and U3	U1	U4

The Perrier unit interpretations are given at the base of the table

in the four units but are scarce in U2 and U3. Only U1 and U4 have jigsaw-fractured blocks. These structures are common and well developed in U4, but are rare in U1. U4 presents various internal structures such as mixed facies injections in blocks, shearing features and local block piles similar to the typical debris avalanche block facies (Glicken 1991).

Taking into account all the field evidence and the discriminatory characteristics (Table 2), we consider that U1 is the deposit of a debris flow, spawned from a debris avalanche upstream and cohesive enough to preserve jigsaw crack blocks. From the observations made, it is not possible to decide an exact origin for this debris flow, but it could be either debris avalanche deposit dam breakout or liquefaction of a debris avalanche during transport. U2 and U3 have clear debris flow deposit affinities and could be the reworking products of U1 or its source, given their lithological content and facies. U4 is a distal debris avalanche deposit with a mixed facies. Partial saturation is observed at the base of the flow probably due to river water incorporation. L1 and L2 were first interpreted as being parts of U4 that infilled palaeoravines, but on closer inspection are clearly found to be later landslides. Thus, they are red herrings in the volcanic succession, confusing the palaeoreconstruction, but providing information on the present day hazards.

Implications for the Perrier sequence

The Perrier units have not been dated precisely, but the Perrier sequence history can be reconstructed using stratigraphy, deposit geometry and textural/structural components (Figs. 4 and 5). It is likely that U1 was emplaced soon after the trachytic plinian fall (RP2 in Pastre 2004) about 2.4 Ma ago as there is little fluviatile reworking affecting this layer and because there are no fluviatile deposits in between. Based on wood voids and clay block deformation, we observed that in one locality, U1 was flowing towards the southeast. This direction possibly indicates the orientation of the palaeo-Couze Pavin river course but it could also be a local artefact due to a meander of the fluvial bed. Conglomerate and sand layers are inter-bedded between all the units. U2 and U3 were emplaced without much fluviatile incision. The slight eastward slope of the conglomerates and sand layers between U1 and U2 could correspond to the Couze Pavin river course. The large amount of pumice in the three debris flow deposits indicates that the activity at the Monts Dore Volcano produced large amounts of pyroclastic material before it collapsed. The unconformity observed between U3 and U4 suggest a prolonged period of fluviatile incision. The shape of this unconformity and the products found on top suggest that prior to U4 emplacement, the eastern part of Perrier Plateau was a terrace of the palaeo-Allier, whereas the western part was probably an alluvial plain with little erosion dominated by deposition of ash and sand. The large amount of tephrite material in U4 is correlated with a period of tephrite extrusion at the Monts Dore Volcano and dated at 2 Ma (Cantagrel and Baudron 1983).

We propose that U1 filled the palaeoconfluence between Couze Pavin and Allier rivers forcing the Allier River to migrate towards the east. Between U1 and U3, the main drainage for the Perrier sector was probably the Couze Pavin River. After a long period of incision, the Allier River returned for the last time to the Perrier sector. U4 was emplaced about 2 Ma ago and forced the Allier river course to move definitively eastwards. This description further refines the interpretation of the late Pliocene Allier River basin history by Pastre (2004).

Landslides and hazard assessment for Perrier

In 1733, a large landslide mobilised the Pardines basanite, part of the Perrier epiclastic sequence and destroyed the Pardines village in 1 day (Vidal et al. 1996). The deposit of this landslide has many similarities to debris avalanche deposits, such as a hummocky topography and a mixed facies. This landslide was partially saturated and had a great mobility (Fig. 10) with a runout of 1,200 m for a vertical drop of 173 m (H/L ~ 0.13). L1 and L2 have the same characteristics as the 1733 deposits (Fig. 10). The sources of L1 and L2 are clearly seen in the field and with aerial photographs. They are located close to large mega-block concentrations in U4 (Fig. 4). L1 runout is not visible due

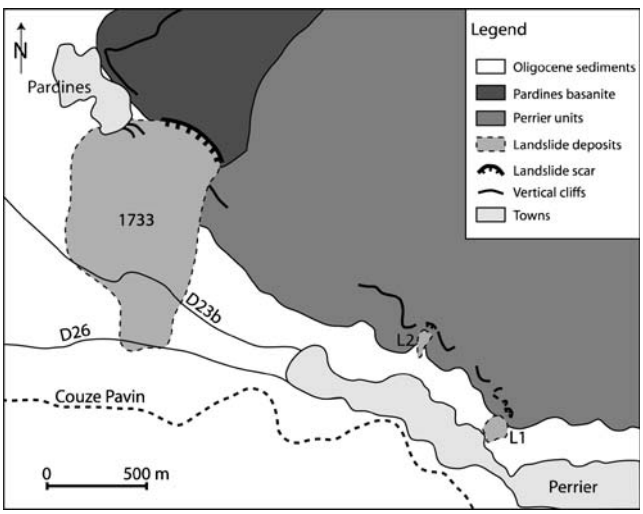

Fig. 10 Simplified geological map of the Perrier Plateau with extent of recent landslides (1733, *L1* and *L2*). The vertical cliffs correspond generally to mega-block areas in U4 and can be the source of future landslides or rockfalls

to the vegetation cover and could be partially buried under Perrier village. L2 reaches at least 200 m from its source, with a vertical fall estimated at 70–90 m (H/L ~ 0.4). No dates are available for these deposits and troglodytic dwellings in the L1 source scarp suggest that L1 is more than a few hundred years old.

Landslides seem to be common on the Perrier Plateau and the village of Perrier could be considered as potentially at risk. The landslide locations are close to concentrations of large tephrite mega-blocks in U4. Such mega-blocks induce structural discontinuities in the epiclastic sequence. At present, vertical cliffs of about 40–50 m high, made of this unstable material, are concentrated near the Marifolet tower (Fig. 3a), with houses within a radius of only 150 m (Fig. 10). We propose two hazard scenarios for the Perrier Plateau. Fall of mega-blocks from the vertical cliffs due to heavy rain, freeze–thaw or moderate intensity earthquake are the most likely hazard. Larger landslides such as the L1, L2 and 1733 events are related to discontinuities in the epiclastic sequence and water accumulation in localised layers, such as the unconsolidated conglomerate and sand layers between U1, U2, U3 and U4. For the 1733 event, the collapse was preceded by the drying out of water wells in 1713 (Vidal et al. 1996). For this reason, unusual precipitation patterns and alteration of the hydrology of the Perrier Plateau may generate instability.

Conclusions

We show that it is possible to differentiate the origin of enigmatic volcanic breccias with detailed deposit facies and structure analysis and assign a debris avalanche, debris flow or mixed ancestry. To make this distinction, a large range of field evidence must be used due to similarities between these products. We emphasise that one event or deposit can transform into another. Debris flows can be derived from debris avalanches or debris avalanche deposits (U1, U2 and U3). Debris avalanches can incorporate debris flow deposits and turn locally into debris flow by liquefaction (U4). New landslides can mobilise debris flow and debris avalanche deposits (L1 and L2), creating a deposit that is very similar to the original. The Perrier sequence allows us to distinguish at least two episodes of sector collapse of the Monts Dore Volcano in the late Pliocene, with (re) mobilisation of the eruptive products in long-runout debris avalanches and debris flows.

Work such as this provides information which is necessary to improve the present database on epivolcanic phenomena, which is clearly useful for hazard assessment. The new palaeogeographic data allow us to improve our knowledge of the Allier River basin and the Monts Dore Volcano. These results also illustrate the great impact that large cohesive debris flow deposits and debris avalanche deposits can have on major drainage systems even 35 km from their source. The present Perrier Plateau has been affected by several landslides and such phenomena may be influenced by the presence of large mega-blocks that induce structural discontinuities in the deposit. Landslides are a potential hazard for Perrier and other deep valleys around the volcano.

Acknowledgements We would like to thank the locals of Perrier for their hospitality and their hard work that has uncovered many outcrops during their restoration work on the troglodyte dwellings. We also want to thanks Daniel Andrade, Silvana Hidalgo and Olimpiu Pop for their help and suggestions in the field. Thoughtful reviews by Lucia Capra and Stuart Dunning improved this paper.

References

Baudron JC, Cantagrel J-M (1980) Les deux volcans des Monts Dore (Massif Central Français): arguments chronologiques. C R Acad Sciences Paris 290(D):1409–1412

Belousov A, Belousova M, Voight B (1999) Multiple edifice failures, debris avalanches and associated eruptions in the Holocene history of Shiveluch volcano, Kamchatka, Russia. Bull Volcanol 61:324–342

Bernard B, Van Wyk de Vries B, Barba D, Leyrit H, Robin C, Alcaraz S, Samaniego P (2008) The Chimborazo sector collapse and debris avalanche: deposit characteristics as evidence of emplacement mechanisms. J Volcanol Geotherm Res 176(1):36–43 Special issue on Ecuadorian volcanism

Calvari S, Tanner LH, Groppelli G (1998) Debris-avalanche deposits of the Milo Lahar sequence and the opening of the Valle del Bove on Etna volcano (Italy). J Volcanol Geotherm Res 87:193–209

Cantagrel J-M, Baudron JC (1983) Chronologie des eruptions dans le massif volcanique des Monts Dore (méthode potassium–argon): implication volcanologiques. Géol Fr I(1–2):123–142

Cantagrel J-M, Briot D (1990) Avalanches et coulées de débris: le volcan du Guéry; où est la caldéra d'effondrement dans le Massif des Monts Dore? C R Acad Sci Paris 311(II):219–225

Capra L, Macías JL (2000) Pleistocene cohesive debris flows at Nevado de Toluca Volcano, central Mexico. J Volcanol Geotherm Res 102(1–2):149–167

Capra L, Macías JL (2002) The cohesive Naranjo debris-flow deposit (10 km3): a dam breakout flow derived from the Pleistocene debris-avalanche deposit of Nevado de Colima Volcano (México). J Volcanol Geotherm Res 117:213–235

Capra L, Macias JL, Scott KM, Abrams M, Garduño-Monroy VM (2002) Debris avalanches and debris flows transformed from collapses in the Trans-Mexican Volcanic Belt, Mexico—behavior, and implications for hazard assessment. J Volcanol Geotherm Res 113:81–110

Chayes F (1956) Petrographic modal analysis—an elementary statistical appraisal. Wiley, London, p 113

Costa JE, Shuster RL (1988) The formation and failure of natural dams. Geol Soc Am Bull 100:1054–1068

Duffell H (1999) Contribution géochronologique à la stratigraphie volcanique de Massif des Monts Dore par la méthode 40Ar/39AR. DEA thesis. University Blaise Pascal, Clermont-Ferrand, p 56

Glicken H (1991) Sedimentary architecture of large volcanic-debris avalanches. In: Fisher RV, Smith GA (eds) Sedimentation in Volcanic Settings, SEPM Spec Pub 45. SEPM, Tulsa, OK, pp 99–106

Glicken H (1996) Rockslide-debris avalanche of May 18, 1980, Mount St. Helens volcano, Washington. Open-file Report 96-677, Cascades Volcano Observatory, Vancouver, p 90

Kerle N, van Wyk de Vries B (2001) The 1998 debris avalanche at Casita volcano, Nicaragua—investigation of structural deformation as the cause of slope instability using remote sensing. J Volcanol Geotherm Res 105(1–2):49–63

Lo Bello P (1988) Géochronologie par la méthode 39Ar-40Ar de ponces quaternaires contaminées. Exemple des ponces du Mont-Dore (Massif Central français). Utilisation d'un laser continu pour la datation de minéraux individuels. Thèse 3° cycle, Université Blaise Pascal, Clermont-Ferrand, p 122

Ly MH (1982) Le plateau de Perrier et la Limagne du Sud : Etudes volcanologiques et chronologiques des produits montdoriens. Thèse 3° cycle, Université Blaise Pascal, Clermont-Ferrand, p 180

McGuire WJ (1996) Volcano instability: a review of contemporary themes. In: McGuire WJ, Jones AP, Neuberg J (eds) Volcano instability on the Earth and others planets. Geol Soc London Spec Pub 110. Geological Society of London, London, pp 1–23

Ménard JJ (1979) Contribution à l'étude pétrogénétique des nappes de ponces du massif volcanique du Mont-Dore. Thèse 3° cycle, Université d'Orsay, Paris, p 105

Mossand P (1983) Le volcanisme anté et syn-caldera des Monts-Dore (Massif Central français), implications géothermiques. Thèse 3° cycle, Université Blaise Pascal, Clermont-Ferrand, p 197

Nehlig P, Boivin P, De Goër de Hervé A, Mergoil J, Prouteau G, Sustrac G, Thiéblemont D (2003) Les volcans du Massif central. Géologues Massif Central: 1–41

Palmer BA, Alloway BV, Neall VE (1991) Volcanic-debris-avalanche deposits in New Zealand—lithofacies organization in unconfined, wet-avalanche flows. In: Fisher RV, Smith GA (eds) Sedimentation in Volcanic settings, SEPM Spec Pub 45. SEPM, Tulsa, OK, pp 89–98

Pastre J-F (2004) The Perrier Plateau: a Plio-Pleistocene long fluvial record in the river Allier Basin, Massif Central, France. Quaternaire 15:87–101

Pastre J-F, Cantagrel J-M (2001) Téphrostratigraphie du Mont Dore (Massif Central, France). Quaternaire 12(4):249–267

Rodolfo KS (1989) Origin and early evolution of lahar channel at Mabinit, Mayon volcano, Philippines. Geol Soc Am Bull 101:414–426

Siebert L (1984) Large volcanic debris avalanches: characteristics of source areas, deposits and associated eruptions. J Volcanol Geotherm Res 22:163–197

Siebert L (2002) Landslides resulting from structural failure of volcanoes. Geol Soc Am Rev Eng Geol XV:209–235

Siebert L, Glicken H, Ui T (1987) Volcanic hazards from Bezymianny- and Bandai-type eruptions. Bull Volcanol 49:435–459

Smith GA, Lowe DR (1991) Lahars: volcano-hydrologic events and deposition in the debris flow-hyperconcentrated flow continuum. In: Fisher RV, Smith GA (eds) Sedimentation in Volcanic Settings, SEPM Spec Pub 45. SEPM, Tulsa, OK, pp 59–70

Ui T (1983) Volcanic dry avalanche deposits—identification and comparison with nonvolcanic debris stream deposits. J Volcanol Geotherm Res 18:135–150

Ui T (1989) Discrimination between debris avalanche and other volcanoclastic deposits. In: Latter JH (ed) Volcanic hazards. IAVCEI Proc. Volcano. Springer, Berlin, pp 201–209

Ui T, Glicken H (1986) Internal structural variations in a debris-avalanche deposit from ancestral Mount Shasta, California, USA. Bull Volcanol 48(4):189–194

Ui T, Takarada S, Yoshimoto M (2000) Debris avalanches. In: Sigurdsson H, Houghton B, McNutt SR, Rymer H, Stix J (eds) Encyclopedia of volcanoes. Academic, London, pp 617–626

Vallance JW (2000) Lahars. In: Sigurdsson H, Houghton B, McNutt SR, Rymer H, Stix J (eds) Encyclopedia of volcanoes. Academic, London, pp 601–616

van Wyk de Vries B, Self S, Francis PW, Keszthelyi L (2001) A gravitational spreading origin for the Socompa debris avalanche. J Volcanol Geotherm Res 105:225–247

Vidal N, Goër De, de Hervé A, Camus G (1996) Déstabilisation de reliefs d'érosion en terrain volcanique: exemples pris dans le Massif Central Français. Quaternaire 7:117–127

Vincent PM (1980) Volcanisme et chambre magmatique : l'exemple des Monts-Dore. Livre du centenaire. Mém Soc Géol Fr 10:71–85

Voight BH, Glicken H, Janda RJ, Douglass PM (1981) Catastrophic rockslide avalanche of May 18. In: Lipman PW, Mulineaux DR (eds) The 1980 eruptions of Mount St. Helens, Washington. U.S. Geological Survey, Washington, DC, pp 347–377

Yarnold JC (1993) Rock-avalanche characteristics in dry climates and the effect of flow into lakes: Insights from mid-Tertiary sedimentary breccias near Artillery Peak, Arizona. Geol Soc Am Bull 105:345–360